

# Radar target stimulation for automotive applications

ISSN 1751-8784  
Received on 28th February 2018  
Revised 2nd May 2018  
Accepted on 14th June 2018  
doi: 10.1049/iet-rsn.2018.5126  
www.ietdl.org

Michael Ernst Gadringer<sup>1</sup> ✉, Franz Michael Maier<sup>2</sup>, Helmut Schreiber<sup>1</sup>, Vamsi Prakash Makkapati<sup>2</sup>, Andreas Gruber<sup>1</sup>, Michael Vorderderfler<sup>1</sup>, Dominik Amschl<sup>1</sup>, Steffen Metzner<sup>3</sup>, Horst Pflügl<sup>3</sup>, Wolfgang Bösch<sup>1</sup>, Martin Horn<sup>2</sup>, Michael Paulweber<sup>3</sup>

<sup>1</sup>Institute of Microwave and Photonic Engineering, Graz University of Technology, Inffeldgasse 12, 8010 Graz, Austria

<sup>2</sup>Institute of Automation and Control, Graz University of Technology, Inffeldgasse 21/B, 8010 Graz, Austria

<sup>3</sup>AVL List GmbH, Hans-List-Platz 1, 8020 Graz, Austria

✉ E-mail: michael.gadringer@tugraz.at

**Abstract:** Automated driving is seen as one of the key technologies that influences and shapes our future mobility. Modern advanced driver assistance systems (ADAS) play a vital role towards achieving this goal of automated driving. Depending on the level of automation, the ADAS takes over the complete or partial control of the movement of the car. Hence, it is mandatory that the system reacts reproducibly and safely in a wide range of possible situations. Especially in complex and potentially dangerous traffic scenarios a test system with the ability to simulate realistic scenarios is required. The authors present an implementation of a vehicle-in-the-loop (ViL) test system which accomplishes these goals in a defined environment. Of the great plenty of sensors stimulated in this context, the radar sensor takes a special position due to its robust and comprehensive information perceiving capability. Stimulating the automotive radar sensor in a ViL environment requires supporting the complex movements of the considered traffic scenarios. For this task, a modular and highly scalable radar target stimulator is necessary, which is capable of stimulating multiple independent moving targets with realistic parameters. The authors are discussing the underlying concepts of the suggested solution and are presenting its performance.

## 1 Introduction

The automotive industry faces its most significant changes in its history: electrification and digitalisation are the new challenges. For a long time each new function in an automobile was implemented as a stand-alone electronic control unit (ECU). This approach quickly proved to be insufficient with the need for functions to be distributed over several ECUs and the need for information exchanges among functions. Today, premier cars have up to 70 ECUs, connected by several system buses [1].

These new technologies merge with classical automotive engineering. Focusing on automated driving among these technologies, it is mandatory, to demonstrate the reliability, safety and robustness in all conceivable situations. Additionally, a goal is to outperform a human driver in steering an automobile and, thus, reducing the number of accidents involving personal injury. Based on the 'Allgemeiner Deutscher Automobil-Club' statistic 2010–2012 a distance of 12 million kilometres between two accidents on German roads was estimated for human drivers [2]. For a risk limited introduction of automated driving a confidence range of the supposed expected values for the accident rate can be derived. After defining an absolute tolerable risk a minimum safety qualification distance of 1–10 million kilometres turned out to be necessary [2, 3]. This can be achieved with a fleet of vehicles, but various factors such as safety, economic feasibility, and ease of reproducibility are of concern. Taking further into account the high number of vehicle variants and software versions, it becomes obvious that new techniques are required for test and validation of these automotive solutions.

Thus, there is an increasing need for a holistic testing method that is as close to reality as possible, while being capable of testing a wide range of traffic scenarios. For this reason, some of these test and validation activities should be moved to a defined environment like an automotive test rig. The vehicle-in-the-loop (ViL) test system able to stimulate the required sensors and actuators is one possible realisation of such a test rig [4]. An example for such a test rig is presented in [4, 5]. This system is located in a large hall

surrounded by remote controlled dummies conducting the movements according to the simulated traffic scenario. Such a huge effort can only be justified by the reproducibility of the test scenarios and the even higher effort of full-scale road tests [6].

Of the multitude of sensors that are stimulated by such a ViL test, the radar sensor takes a special position. On the one hand, radar sensors are robust against environmental factors (such as rain, fog, snow), which makes them a very important sensor in many present and future systems. On the other hand, it is challenging task to generate radar echoes in real-time for complex traffic situations as required for ViL testing. One possibility of realising the radar echoes is to use movable dummies in front of the radar sensor as mentioned before [4]. If the requirements on space and effort of such an implementation are not viable, an (electronic) radar target stimulator (RTS) must be considered [7–9].

Within this article we introduce concepts and structures for realising an RTS used in a ViL environment focusing on the testing of automated driving functions. In Section 2, we provide an overview of the requirements of RTS systems. In this regard existing implementations of RTS systems are grouped according to their usage and application within the automotive sector. Thereafter, we give a summary on a ViL system in Section 3. In this context, we discuss the partitioning between the environment simulation (ES) and the underlying hardware.

The ES covering the driving dynamics is an important component of the ViL software platform. This simulation supplies all information of the different objects participating in the driving scenario. In Section 4, we present the extraction of the parameters relevant for the radar sensor from this information. Subsequently, we introduce the concepts of our hardware implementation in Section 5. The following section provides a performance overview of the presented RTS system. Finally, in Section 7, we summarise this article with a brief conclusion.

## 2 Radar target stimulation systems

### 2.1 Automotive radar

Automotive radar sensors have undergone quite an evolution since radar was first used in cars. While originally pulsed systems at 24 GHz were used, this changed on the one hand to frequency modulated continuous wave (FMCW) radars and on the other hand to the 77 GHz band. Besides technical reasons (higher bandwidth) the latter was forced by legislative regulations since the 24 GHz band will be phased out for radar usage by 2022. The future trend goes even to frequencies above 100 GHz [10].

Another major development regarding the design of automotive radars concerns the antenna and the beam forming. At the beginning mainly mechanically steered antennas were used. The actual generation of radars applies patch arrays with electronic beam steering or digital beam forming.

Modern radars use a sophisticated set of waveforms, receiver structures and signal processing algorithms to acquire reliable and high-resolution radar target information in a crowded electromagnetic environment with a large number of potential interferers. Currently automotive radars mainly use FMCW waveforms with bandwidth between 250 MHz and 1 GHz for long-range sensors and up to 4 GHz for short-range sensors to provide a high-range resolution. In combination with correlation receivers, the energy of signals which does not match the transmitted waveform is spread over a large bandwidth and, therefore, unwanted signals are effectively suppressed [11]. Following the receiver the radars perform coherent signal processing to determine range and velocity of a target. This processing step also suppresses non-coherent targets since their phase relations are random and therefore the signal energy is spread over multiple Range–Doppler bins [12]. In a last step, the detected targets and their estimated parameters are fed into a tracking algorithm, which performs plausibility checking of movement and size changes to physical models. All targets which show a non-physical behaviour at this stage (e.g. change of range is not related to Doppler information) are suppressed.

### 2.2 Fundamentals of radar target stimulation

The task of the RTS is to stimulate a radar sensor in such a way that it ‘sees’ virtual – non existing – targets undistinguishable from real objects (‘deceptive jamming’, [12]). To accomplish this, the transmitted radar waveform has to be sent back to the radar with the following modifications:

- delay corresponding to the target range,
- frequency is shifted according to the relative velocity of the target,
- attenuation or amplification depending on the target's radar cross section (RCS) and distance.

The stimulation parameters are given by the following equations, where  $\tau$  is the required time delay,  $R$  is the target distance,  $c_0$  is the velocity of light,  $f_D$  is the Doppler frequency shift,  $v$  is the difference of the radial velocities (range rate),  $f_0$  is the radar frequency,  $G$  is the necessary amplification of the transmit power in order to stimulate the intended RCS at a given distance. In this context,  $\sigma$  expresses the RCS of the target:

$$\tau = \frac{2R}{c_0} \quad (1)$$

$$f_D = \frac{2vf_0}{c_0} \quad (2)$$

$$G \propto \frac{\sigma}{R^4}. \quad (3)$$

To be able to generate convincing targets for such a sophisticated radar sensor as described in Section 2.1 is a very demanding task and requires special attention to the system architecture and the

deceiving techniques used. The first important point is to choose a suitable system architecture to ensure the coherence of the modified radar waveform. To achieve this goal, suitable methods are either to perform all processing stages directly in the radio frequency (RF) range of the radar (e.g. in the 24 GHz or 77 GHz range) or to convert the RF signal into a suitable intermediate frequency (IF) range. In this case, the RTS has to use the same local oscillator (LO) for the down- and upconverter, otherwise small frequency and phase deviations of the LOs will degrade the coherence of the generated target signal.

The second critical issue is the processing of the large bandwidth waveform with its unpredictable modulation characteristics. To cope with this issue, the RTS needs to be able to process the full bandwidth of the transmitted waveform on the fly, otherwise the target will be discarded in the correlation receivers of the radar. This behaviour prohibits the usage of the ‘estimate-and-synthesise’ and ‘store-and-replay’ modes of digital radio frequency memory (DRFM) [12]. DRFMs can, therefore, only be used in the stream processing mode, which is only suitable for large target distances (e.g.: usually >30–100 m) due to the inherent delay of analogue-to-digital converters (ADCs), digital-to-analogue converters (DACs) and processing algorithms. Since the realistic stimulation of automotive radars also requires to cover closer ranges a suitable analogue solution has to be included.

The third point to be covered is techniques generating targets which can pass through the physical plausibility checks of the tracking algorithms in the radar sensors. A suitable approach is the use of coupled range and velocity gate pull-off, which ensures that the range change rate and the Doppler information are always correlated. While a physical range change of the target is relatively easy with the help of mechanical simulations, digital control algorithms and fine resolution delays, the application of a small Doppler-shift (e.g. several kHz Doppler-shift) onto the radar signal with its large bandwidth (e.g. several hundred MHz) is a very demanding task. Additionally, the RCS of the target has to be modified according to the range change, otherwise the target will get larger with growing distance which is an unnatural behaviour and will be discarded. For more sophisticated radars also the generation of spatial dimensions (coverage of multiple range gates) and statistical RCS fluctuations will be necessary to generate convincing targets.

### 2.3 ViL-testing requirements

In addition to the demands due to the radar sensor itself, given in Section 2.2, further requirements are imposed by the intended integration into a ViL test system:

- Simulating complex driving scenarios within the ViL test requires the RTS stimulating multiple targets moving in arbitrary directions.
- Focus on short target distances down to about 2 m
- Over-the-air (OTA) testing of the radar sensor
- The RTS shall not use any a priori knowledge about the radar sensor and especially its waveform.

The impact of these requirements on the design of our RTS will be discussed in Section 5.1.

### 2.4 RTS systems for automotive applications

Sections 2.2 and 2.3 highlighted demanding requirements for the RTS equipment integrated into a ViL test system. Several applications in the automotive area do not require this comprehensive focus. One important group of RTS is designed for ‘end-of-line’ testing of radar sensors. The goals for this task are the verification of electrical properties of the sensor as well as confirming that the sensor can detect an object under given conditions. This type of test can be performed conducted (i.e. the test equipment is directly connected to the sensor) or as an OTA test. Conducted tests are often used to check sensors which are not fully assembled while OTA tests are conducted using the final product. The ‘end-of-line’ RTS test systems often stimulates only

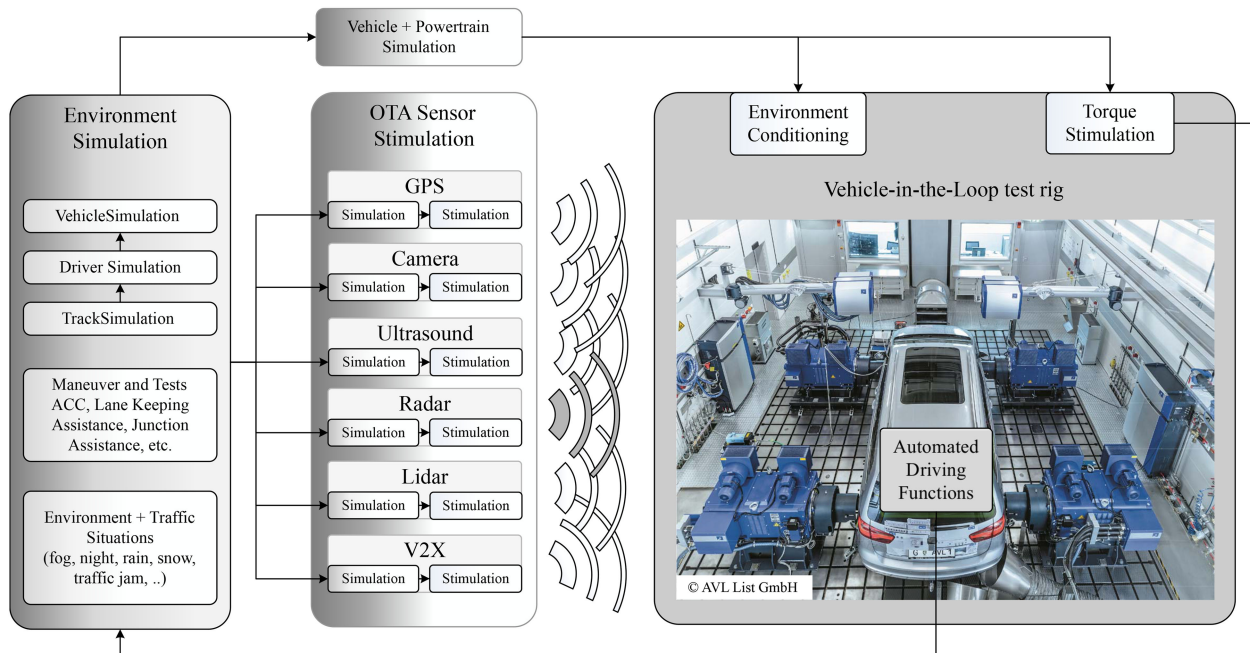


Fig. 1 Driving-Cube test bench for holistic testing of automated driving [6, 22]

one non-moving target at a few given distances. By applying a Doppler-shift to the radar transmit signal a velocity of the target is emulated. Due to the reduced complexity of the ‘end-of-line’ RTS equipment, these systems are often characterised by a fast measurement speed and a comprehensive electrical performance. Manufacturers of such test equipment are [13–16].

To test advanced driver assistance system (ADAS) functionality under laboratory conditions an RTS must stimulate at least one target of which the distance is changed electronically based on the test scenario. Usually, the distance of the moving targets is varied at a fixed angle seen by the radar sensor [15, 17, 18]. To realise also an azimuthal movement of a target a rotation of the sensor [19], a movement of the antennas of the RTS [8, 20], or a movement of the full RTS equipment [21] was implemented by the different manufacturers.

### 3 ViL testing for automated driving functionality

As summarised in Section 1, the increasing complexity of modern vehicle concepts requires new methods to integrate simulation and test on each level of the validation chain. Especially for the development of ADAS, the interaction between the car and the environment is very important and must be considered in detail [6]. A ViL concept bridging the gap between conventional hardware-in-the-loop and real road testing was developed by AVL List GmbH (AVL), named ‘DrivingCube’ [22], as shown in Fig. 1. In addition to the mechanical input (torque, steering force), also the ADAS-related sensors (camera, radar, lidar etc.) are stimulated over the air.

For these sensor stimulations, it is mandatory to avoid removing the sensors from their location in the car body. If the radar sensor is not stimulated over-the-air, it would be taken out of the loop by direct stimulation of the communication line (usually via the controller area network-bus). In this case, the impact of all parasitic reflections caused by the surrounding elements of the radar sensor, like the bumpers [23], is neglected. Hence, the clutter recognised by the radar sensor during real road testing and, in this way the detected objects, could be different from ViL testing.

For a proper ViL test, significant effort must be spent avoiding interactions between the stimulators of the different sensors. Furthermore, all stimulators must be synchronised to enforce the desired reactions of the ECUs.

The central component of the DrivingCube concept is the ES [24]. It performs the calculation of the traffic scenario including the environmental conditions as well as the mechanics of the movement of the car. This provides the input for the different

sensor stimulation units as well as for the vehicle and power train simulation. The ECUs will take actions based on the gathered sensor information and these actions are fed back to the ES. As all the different stimulation signals depend on the reaction of the vehicle a replay of previously recorded sensor signals is insufficient for this test concept.

In the following, we are discussing the concepts used to include an RTS system into the ViL test system as mentioned before.

### 4 Radar signature generation

The specification summarised in Sections 2.3 and 3 provides the requirements for implementing the radar sensor stimulation for the described application. To achieve this goal, a connection between the ES and the RTS system is needed, as shown in Fig. 2. Using this information, the connection between the objects considered by ES (i.e. car, pedestrian etc.) and the scattering of the waves emitted by the radar sensor (of the ViL) must be established. This scattering information must undergo a mapping process to satisfy the capabilities of the RTS. Thus, the RTS provides the information of the surrounding object to the radar sensor by mimicking their wave scattering. Based on this response the radar sensor calculates a list of objects and sends it to the ECUs of the vehicle. The decisions of the ECUs are then communicated back to the ES allowing for a closed loop testing as shown in Fig. 1.

To implement the described ViL testing we had access to the ES solutions along with the interfaces between ES and test rig, which are available at AVL [24]. Hence, the tasks we had to accomplish in order to realise the described testing concept were radar signature generation (RASIG) based on ES, the mapping of the derived radar signatures on the capabilities of the RTS hardware, and the RTS hardware itself. In the following, we provide an overview of the ideas used to implement RASIG.

As mentioned above, RASIG computes how the electromagnetic waves (EM-waves) originating from the sensor propagate, interact with the objects and return back to the radar sensor. Using the information read from the ES software [24] the 3D traffic scenario is reconstructed within RASIG and the radar wave propagation, interaction with the reconstructed geometry is simulated. For this purpose, the shooting and bouncing ray (SBR) method [25] which is proven to be a very useful tool for asymptotic field computations was chosen. In SBR, a set of rays, representing an EM-wave, are shot into the 3D scene. When a ray hits an object, the calculated distance between the so-called hit point and the ray source is used to account for the well-known quadratic power density reduction due to propagation. The interaction of the

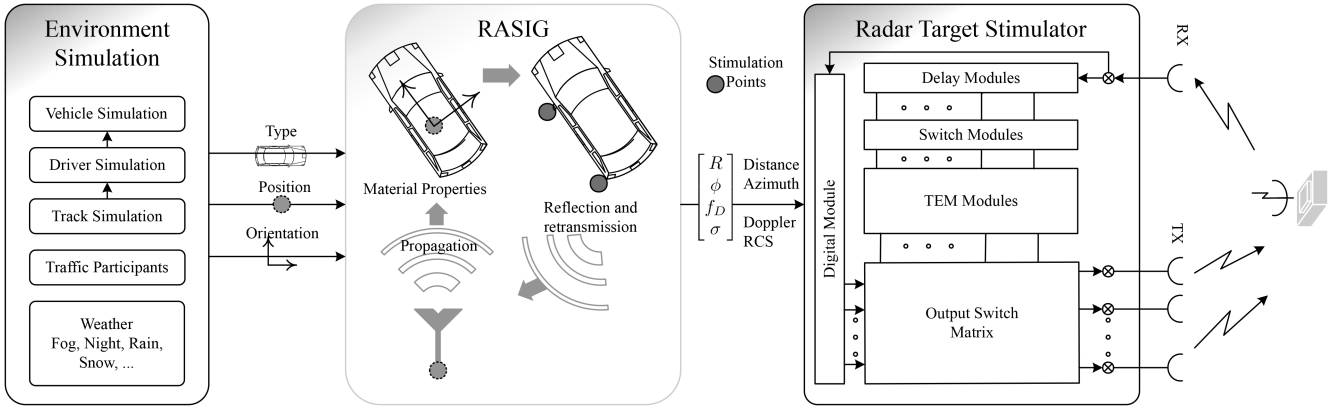


Fig. 2 Concept diagram for radar sensor stimulation with ViL

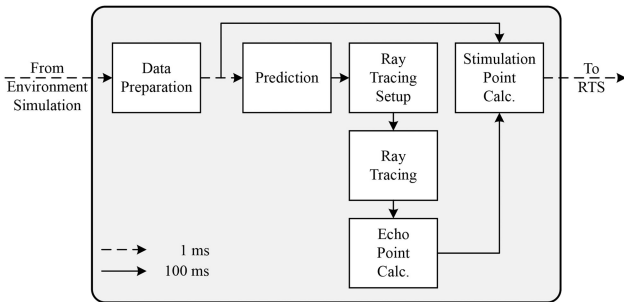


Fig. 3 Block diagram showing the idea of prediction



Fig. 4 Scattered power density for a vehicle geometry

incident EM wave with the hit surface is an important part of RASIG and has been studied extensively. It is dependent on surface size, surface and material properties (roughness, permeability  $\mu$ , and permittivity  $\epsilon$ ) and spatial attributes of source (and this, orientation of polarisation), observer and surface. The so-called bidirectional reflection distribution function (BRDF) is used to compute the reflection towards the observer. One such BRDF, the Phong reflection model [26] proposed in the field of computer graphics is chosen and adapted into the radar field. This adapted Phong BRDF has been normalised and analytically proven to fit with the RCS results (RCS is calculated by considering the ratio of the power density reflected to the power density incident) for a sphere [27]. Advantages of using this approach are: material types can be handled by parametrising the BRDF and computationally efficiency. Another very important advantage of the SBR approach is its suitability to compute multipath propagation. When a ray is incident upon a surface, first the reflected power density is calculated and then a new ray is shot into the specular direction and when this new ray hits another surface the process is repeated again until a termination condition is met. This enables multipath effects to be taken into account which are an important source of various classification errors in radar sensors [28]. After the ray tracing and reflection computation run, a heap of hit points along with their contribution to the reflected field together representing the so-called radar signature is available. For the purposes of stimulation, these hit points need to be grouped into distinct ‘echo points’. Each echo point has the following characteristics: RCS, Doppler shift and position in space. As the RTS provides limited stimulation capabilities only a few echo points are chosen for stimulation, the

so-called stimulation points. This ability to choose stimulation points from echo points based on hardware greatly aids in the scalability of the solution.

RASIG is implemented on NVidia graphics processing unit (GPU) so as to reap the benefits of parallel processing. Even so the computations for RASIG take up to 100 ms. However, in order to stimulate the radar sensor in a way that the object tracking algorithms are not affected, it is required to stimulate every 1 ms. In order to circumvent this problem, the state information of the traffic participants (received at 1 ms rate from ES) are predicted into the future and RASIG is done with this predicted data. Between two prediction steps, the calculated echo points are simply moved according to the new information from the ES. Fig. 3 shows this idea in the form of a block diagram. The result of RASIG on a vehicle simulated using NVidia GPU is shown in Fig. 4. The colour of each pixel represents the corresponding amount of power that is returned towards the observer. The flat surfaces that are oriented normal to the incident field reflect a lot more than the surfaces that are oriented at an oblique angle. As previously mentioned, the results for geometrical entities like a sphere are validated analytically, and it is planned to validate the results for arbitrary 3D shapes, Fig. 4 against real-world measurement data.

The ability to handle different material types, different surface conditions combined with the possibility to consider multipath propagation effects into RASIG contribute to the challenge of the stimulation being realistic. Use of GPU together with the idea of using prediction help in fulfilling the real-time capability challenge.

## 5 Concept and design of the RTS

### 5.1 Concept

The requirement given in Section 2.3 (especially the minimum target distance and the absence of a priori information) demand an analogue implementation of the RTS because we could not identify any civil available signal processing hardware with such short delays (e.g.  $<13$  ns for a distance of 2 m) that would allow real-time processing. Due to the requirement that no a priori knowledge about the sensor is available we cannot record the radar's transmit waveform and do a playback.

The complexity of the analogue implementation increases linearly with the achievable target distance and the number of targets. Therefore an analogue-only system cannot easily cover the whole range of an automotive radar with target ranges up to 300 m. Although the initial requirement focused on short ranges, it is obvious that a usable system has to cover also the long distances. This led to a hybrid (analogue and digital) concept with the switch-over at about 30 m.

To cover the different frequency ranges of automotive radar sensors (see Section 2.1), we decided on the use of an IF processing. We choose the band around a centre frequency of 2 GHz (the IF of the RTS) because of the availability of components on the one hand and the achievable bandwidth on the other hand.

The following sections address some special issues and interesting design choices.

### 5.2 Delay line module

The typical method to achieve variable delays with minimum effort is the use of binary stepped switchable delaylines. For the stimulation of multiple targets one would also need the corresponding number of such delaylines which is a badly scaling design. Our concept is a tapped delayline consisting of a chain of constant non-switchable delays with taps after each single step of delay (see Fig. 5). Of course the delays have to provide for the fact that the radar signal travels twice the target distance. In the case of our RTS, a single step has a delay corresponding to a target distance of about 0.5 m. This is a quite extensive solution but it allows to achieve multiple different delays simultaneously.

While for the first demonstrators we are using coaxial cables to achieve the delay, this will be changed in future designs to delay lines which can be better integrated to printed circuit boards (e.g. defective-ground-structure transmission lines). A photo of a single delay line module is given in Fig. 6.

The connection from a given delay to the target emulation module (TEM) is accomplished by a switch matrix. Fig. 7 shows this concept and its scalability. This scalability allows to adapt the RTS to the requirements of the user both in the range to be covered and the number of targets to be stimulated. Movement of the target

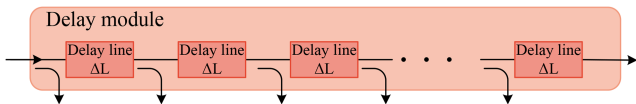


Fig. 5 Scheme of a delay line module

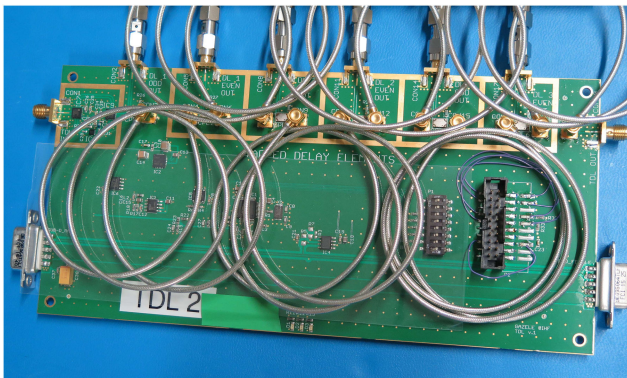


Fig. 6 Single delay line module

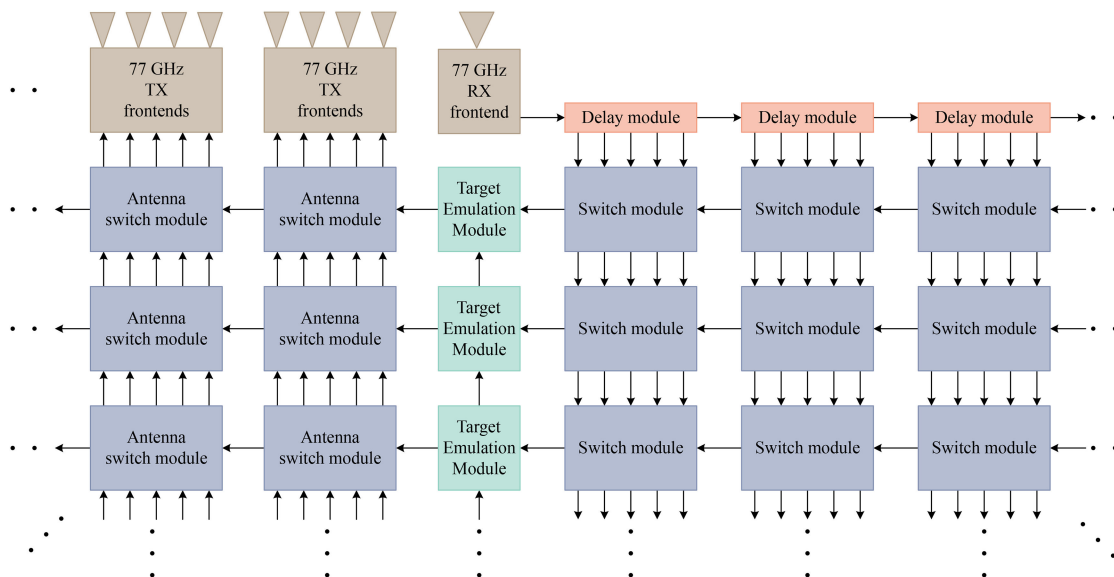


Fig. 7 Concept & scalability of the analogue RTS

can be achieved by switching the TEM from one tap to another one. Since the delay switching is not done at the radar frequency but at a much lower IF the phase change due to the change in distance is not the same as that of a real moving target (see (2) – the Doppler shift depends on the signal frequency  $f_0$ ). The necessary Doppler frequency shift has therefore to be addressed by the TEM.

The switch matrix is designed in a way that it not only allows the one-to-one routing of a tap to a TEM but also to feed the same delay to multiple TEMs and even multiple delays to a single TEM. The latter has the advantage to allow the generation of targets with spatial extension as described in Section 2.2.

### 5.3 Target emulation module

The TEM is responsible to adjust the received radar signal in such a way that the target properties velocity and RCS are correctly detected by the radar. This makes it necessary to have one TEM for each target to be stimulated.

The target's relative velocity, resp. the corresponding Doppler frequency-shift, is provided by a vector multiplier. The challenge was to find a modulator with a bandwidth of about 1 GHz. It has actually been the availability of such a device which has been one determining issue for the choice of the IF range. The I/Q-input signals of the modulator are provided by a digital synthesiser which makes it possible to not only provide single frequency signals but also signals with a more realistic spectral spread.

The signal's amplitude and such the target's RCS are adjusted by digital attenuators.

Besides that, the TEM allows also to set the target's distance with a resolution better than the distance of the taps of the delay line module by a factor of 4 which helps to drastically reduce the

hardware complexity of the delay line and the switch matrix.

Switching either between the taps of the delay line module or between the sub-delays on the TEM itself can cause phase jumps of the signal. To avoid these jumps having an adverse influence on the radar's signal processing, we designed the switching in a way to circumvent this possible problem. The output signals of two neighbouring delays (from the delay line module) are fed simultaneously to the TEM. As shown in Fig. 8, single pole double through (SPDT) alternation switches connect either the 'delay' or the 'delay +  $\Delta L$ ' inputs to the corresponding variable attenuator. The arrangement of delays and switches at the TEM is a simplified version of the delay line and switch matrix setup described in the last section. The purpose of the variable attenuators is to switch between the different delay taps located at the TEM. As these variable attenuators allow a precise control of their input signals we can avoid a hard switching between the delays. Instead we

implemented a soft hand-over between two delays where the signal of the last delay is reduced by the same degree the signal of the next delay is enlarged. As soon as the variable attenuator turned off the signal of its delay tap the corresponding SPDT can switch to the alternative input of the delay line module. By this zero amplitude switching approach phase jumps due to the switching between the taps of the delay line module as well as the taps on the TEM are prevented.

As an example for the performance of the TEM Fig. 9 shows its measured transfer function (respectively the gain of the module and its group delay). In this figure, the bars behind the traces indicate the bandwidth of 1.2 GHz over which the TEM is typically used. Over this frequency range we accomplish a variation of the TEM gain of 2.6 dB. Within these limits, the group delay shows a variation of 840 ps. This progression of the group delay corresponds to a range variation of  $\sim 14$  cm.

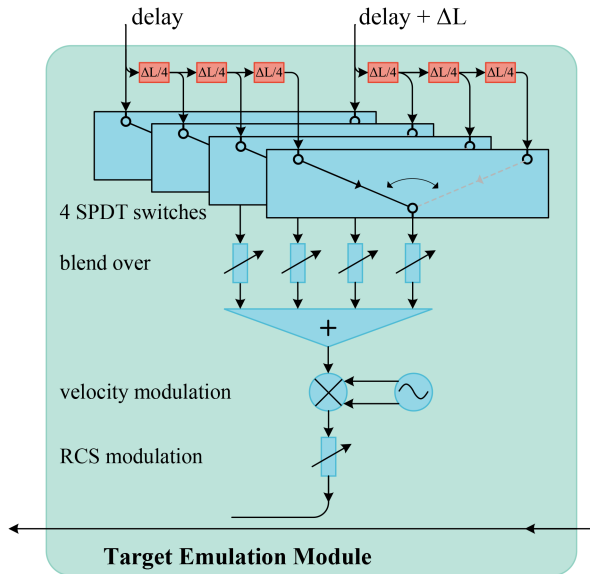


Fig. 8 Scheme of the TEM

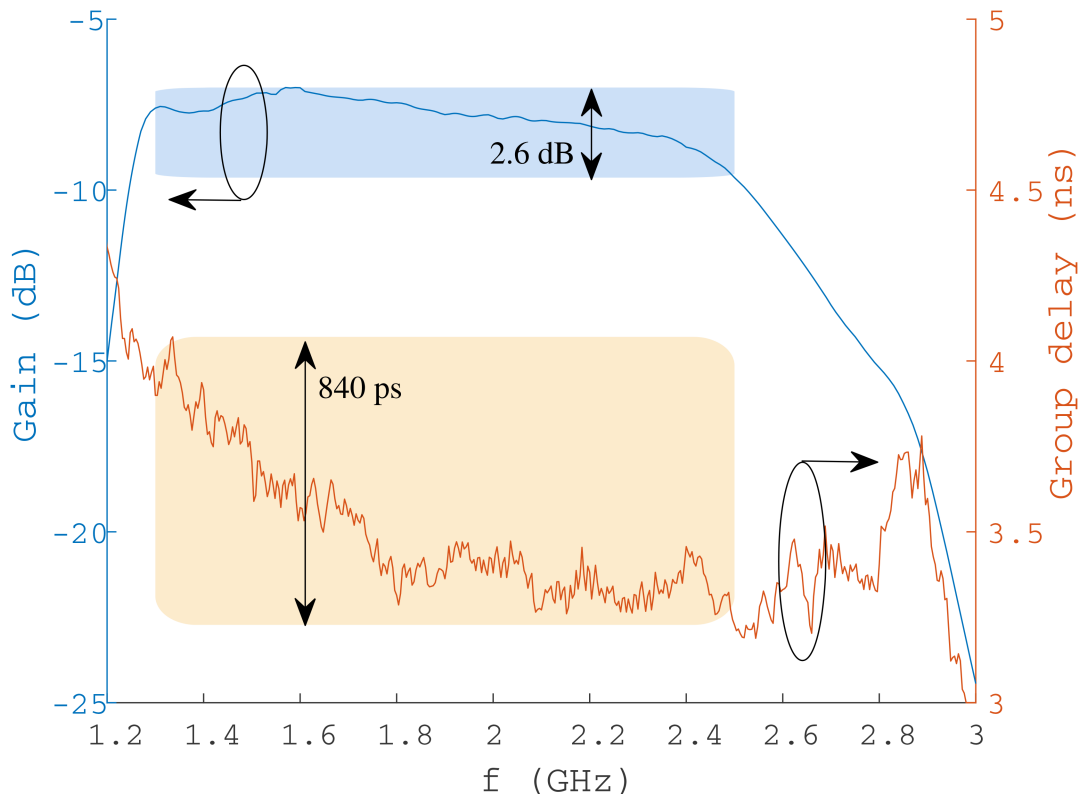


Fig. 9 Measurement results of a TEM. The blue trace shows the gain of the module (left y-axis). The red trace indicates the group delay (right y-axis). The bars behind the two traces indicate the variation of the corresponding measurement parameter over the considered bandwidth of 1.2 GHz

The TEM itself is shown in Fig. 10.

#### 5.4 Antenna switch module

In order to set the azimuth position of a target, we need a set of antennas at different angles. The antenna transmitting the output signal of the RTS back to the radar determines the perceived target's azimuth. The RTS has to be capable to switch dynamically between the antennas to stimulate a smooth lateral movement of the object.

Similar to the switch matrix between the delay line and the TEMs there is a similar switch matrix before the antenna array which routes the output signal of a TEM to the selected antenna (see Fig. 7). It allows both multiple targets (from different TEMs) at a single direction and a single target at multiple azimuth angles making it possible to generate targets with a lateral extent which will be especially necessary for near objects.

#### 5.5 Digital target stimulation

In order to minimise the amount of analogue hardware the analogue RTS is complemented by a digital counterpart. In the AV104 (see Fig. 11) by ApisSys [29], we found a state-of-the-art module with a high-capacity field-programmable gate array (FPGA) possessing, with 180 ns, one of the lowest latency values available on the civil market. This latency corresponds to a minimum target distance of 27 m.

The digital RTS is capable of processing signals with a bandwidth of up to 1 GHz which is about the same as the analogue RTS can achieve. The bandwidth is limited by the sample rate (identically for both ADC and DAC) and the necessary digital finite impulse response (FIR) filters.

The firmware of the digital stimulator is based on a classical DRFM architecture in stream processing mode. As the first step, the digitised signal is converted into the digital baseband with an LO of the frequency  $f_s/4$  and a FIR halfband lowpass filter. This filter is also responsible for most of the processing delay inside the FPGA, since quite a lot of taps are needed to achieve the required stopband attenuation and transition steepness.

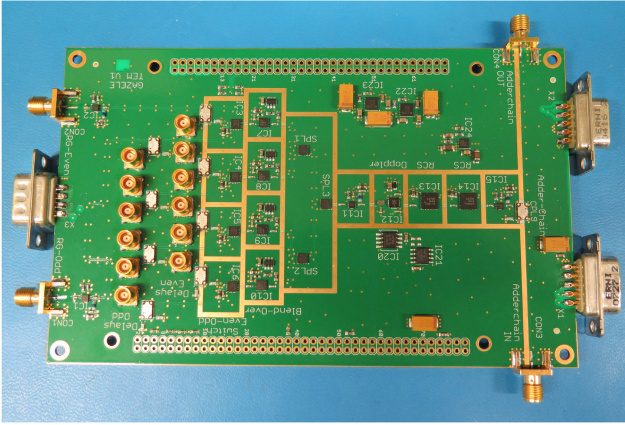


Fig. 10 Single TEM

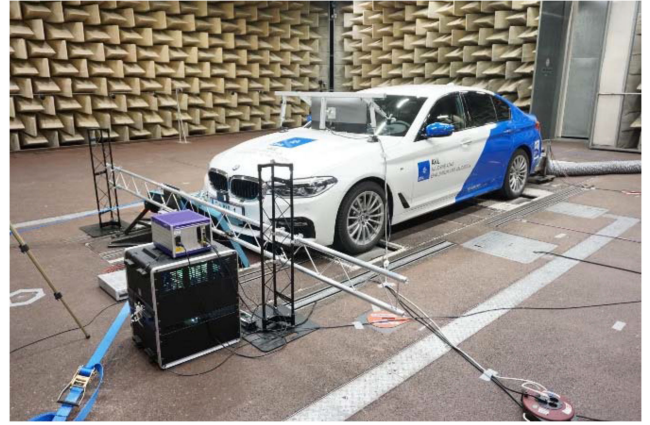


Fig. 13 Setup of the testbed

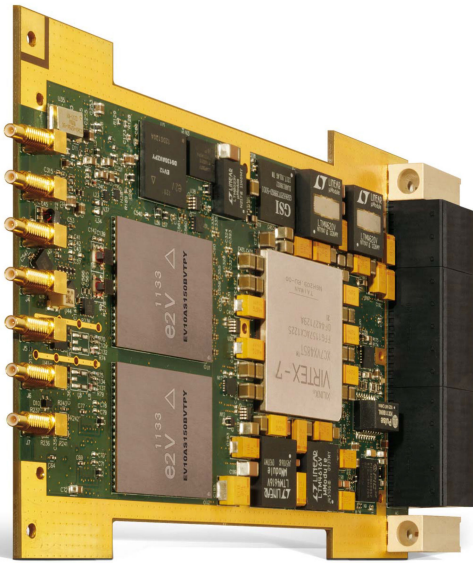


Fig. 11 ApisSys AV104 module (courtesy of ApisSys)

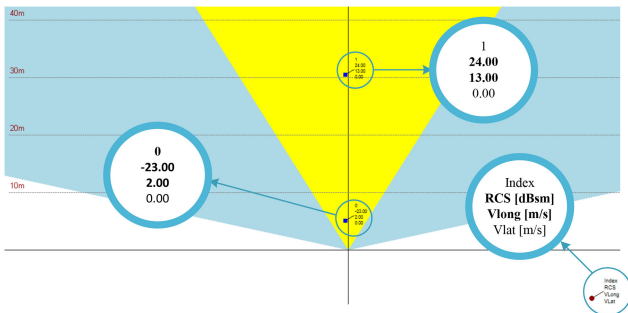


Fig. 12 Stimulation results of laboratory tests

Afterwards the baseband signal is duplicated for each realised target and feed into a complex mixer for the Doppler shift. Since the sampling rate inside the FPGA is significantly lower than the ADC sample rate we need to process several samples in parallel to achieve the required throughput. Therefore, the numerically controlled oscillator and mixer are realised in the form of a parallel polyphase architecture. After the Doppler shift, the signal is converted back into a real signal, which helps us to save valuable FPGA resources for the following processing steps. In the next step, each target implements an independent delay line with a block RAM of the size of 96 kbit configured as a programmable shift register. This delayline is designed to provide a resolution of one sample which is equivalent to a range resolution of around 5 cm. Targets which should have a spatial dimension can be generated by adding up several delay line outputs with a structure similar to an FIR filter.

Of utmost importance for the digital control logic is that the stimulated Doppler frequency-shift and the range-rate are always consistent as already mentioned in Section 2.2 for automotive applications. In the next step, each target uses a multiplier to set the required power level to achieve the desired RCS and channel model. If we use more sophisticated algorithms as the source of this RCS multiplier we are also able to stimulate statistical RCS models and complex surface structures of a desired target. With the above-mentioned resource requirements, the FPGA of the AV104 has a theoretical capability to stimulate up to 30 different targets.

After all targets are processed the resulting samples are added together and sent to the output DAC. In comparison to the ADC, which only needs to process a very limited dynamic range given of the input waveform, the DAC has to provide a sufficiently large dynamic range resulting from the RCS range and the path loss.

Currently, the module is equipped with only a single DAC channel. Therefore we are only able to stimulate targets at one azimuth direction. Of course multiple targets in the same direction can be achieved and this direction can also be dynamically steered. To enable the stimulation of multiple independent azimuths, an update with multiple output channels is planned. These output channels will be connected to the antenna switch matrix in the same way as the analogue TEMs (see Section 5.4).

## 6 RTS system tests

The RTS system has been tested with real radars – ARS 308 and ARS 408 from continental. Those tests have been conducted both under laboratory conditions and on a chassis dynamometer test bench of AVL.

In the former, we observed the stimulated target objects with a software by continental. An example of its display with two targets is shown in Fig. 12. In this test, we could proof that our architecture and its implementation performs as intended. The analogue RTS is able to stimulate two independent targets in the range from 2 to 30 m with an RCS dynamic range of 50 dB. The digital RTS covered the range from 30 upwards to 300 m. We could also show that moving targets provided by the RTS were accepted and correctly detected in the radar's object mode which includes tracking processing.

In case of the testbed both the car's radar sensor and camera were stimulated (see Fig. 13). The data for the stimulations were provided by an ES with feedback of the car's velocity. The testbed and the stimulators were controlled by AVL's Model.CONNECT software. The upper part of Fig. 14 shows the cockpit with a display presenting the fused information from both sensors. In front of the windscreen is a curved monitor for the camera stimulation. This test demonstrated that the RTS can be integrated into the testbed. We were also able to remove the clutter of the surrounding by the use of plates with radar absorbing materials.

## 7 Conclusion

In this article, we presented a strategy for integrating an RTS into a VIL test system focusing on automated driving. The requirements



Fig. 14 Stimulated drive on the testbed

for this integration were derived from the radar sensor as well as from the ViL perspective. Most importantly, the OTA stimulation of the radar sensor, the support of complex traffic scenarios even at short distances and avoiding a prior knowledge of the radar should be mentioned in this context.

These specifications influenced the implementation of both the extraction of the radar stimulator parameters from the object list provided by the ES and the hardware structure. This extraction process, discussed in Section 4, reconstructs the 3D traffic scenario by mapping a shape and material properties onto the objects provided by the ES. Thereafter, a ray-tracing analysis approach is used to derive the wave scattering at these objects. The outcome of this analysis is grouped to extract echo points which constitute the input for the RTS hardware.

The structure of the hardware implementation, as summarised in Section 5, is divided into the analogue and the digital part. In the analogue section, the stimulation of targets in the vicinity of the sensor is implemented. The digital RTS part handles targets positioned far away from the radar sensor. In both cases, emphasis was put in a concept, scalable in the number of supported targets as well as in distance. After merging the outputs of both parts, the signals are sent back to the radar sensor via the antenna switching module. Using this module an azimuthal movement of the stimulated objects is introduced. The complexity of the implementation of the analogue stimulator section is influenced by the latency and processing speed of the digital part. The better these two parameters are the shorter is the distance for the handover between the two parts.

The discussed RTS was incorporated into a ViL testbed provided by AVL. In this test environment, the ES is providing the object information. Based on this information, we validated the ability of the RTS stimulating objects detected and tracked by the radar sensor located in the vehicle. By showing this functionality a further step in the direction of testing automated driving in a ViL testbed was taken.

## 8 Acknowledgments

This work has been partially conducted within the ENABLE-S3 project which received funding from the ECSEL Joint Undertaking (grant no. 692455). This joint undertaking was supported by the European Union's Horizon 2020 Research and Innovation Programme and Austria, Denmark, Germany, Finland, Czech Republic, Italy, Spain, Portugal, Poland, Ireland, Belgium, France, the Netherlands, United Kingdom, Slovakia, and Norway. Additionally, this work was also funded by the Austrian Research Promotion Agency (FFG) under the research project GAZELE (grant no. 848457).

## 9 References

- [1] Rajeshwari, H., Geetishree, M., Gurumurthy, K.S.: 'An insight into the hardware and software complexity of ECUs in vehicles'. Advances in Computing and Information Technology, Chennai, India, July, 2011, 56, pp. 99–106
- [2] Schnieder, S.: 'How to measure/calculate radar system MTBF?'. European Radar Conf., Workshop: Automotive Radar Measurement Solutions – For End-of-Line Purposes as well as in Aftersales, Nuremberg, Germany, October 2017, pp. 1–24
- [3] Koopman, P., Wagner, M.: 'Challenges in autonomous vehicle testing and validation'. SAE World Congress, Detroit, MI, USA, April 2016, pp. 1–10
- [4] Gietelink, O., Ploeg, J., De Schutter, B., *et al.*: 'Development of advanced driver assistance systems with vehicle hardware-in-the-loop simulations', *Veh. Syst. Dyn.*, 2006, 44, (7), pp. 569–590
- [5] 'Grand Cooperative Driving Challenge': 'Youtube movie demonstrating the concept (relative motion) of the VeHIL (vehicle hardware-in-the-loop) facility', Available at [https://www.youtube.com/watch?v=HQT\\_8JAqro](https://www.youtube.com/watch?v=HQT_8JAqro), accessed February 25, 2018 December 2009,
- [6] Schyr, C., Brissard, A.: 'Drivingcube – a novel concept for validation of powertrain and steering systems with automated driving functions'. Int. Symp. Advanced Vehicle Control, Munich, Germany, September 2016
- [7] Nelson, R.: 'Radar gives cars eyes', EDN Network, Available at <https://www.edn.com/design/test-and-measurement/4380245/Radar-gives-cars-eyes>, accessed February 25, 2018, May 2002
- [8] Graf, S., Roßmann, M.: 'OTA radar test for autonomous driving based on a 77 GHz radar signal simulator'. European Radar Conf., Workshop: Automotive Radar Measurement Solutions – For End-of-Line Purposes as well as in Aftersales, Nuremberg, Germany, October 2017, pp. 1–19
- [9] Gruber, A., Gadringer, M., Schreiber, H., *et al.*: 'Highly scalable radar target simulator for autonomous driving test beds'. European Radar Conf., Nuremberg, Germany, October, 2017, pp. 147–150
- [10] Meinel, H.H., Dickmann, J.: 'Automotive radar: from its origins to future directions', *Microw. J.*, 2013, (9), pp. 1–9
- [11] Pace, P.E.: 'Detecting and classifying low probability of intercept radar' (Artech House, Boston London, 2008), ISBN: 978-1-59693-234-0
- [12] Adamy, D.L.: 'EW104: EW against a new generation of threats' (Artech House, Boston London, 2015), ISBN 978-1-60807-869-1
- [13] W.K.S. Informatik GmbH.: 'Radar target simulator 24 GHz and 77 GHz', Available at <http://www.wks-informatik.de/en/solutions/radar-target-simulator>, accessed February 25, 2018]
- [14] Keycom Corp.: 'Passive radar test system', Available at <http://www.keycom.co.jp/e/products/rat/rat09/page.html>, accessed February 25, 2018
- [15] Rohde & Schwarz.: 'Excellence in precision solutions of automotive radar'. Solution Brochure, November 2017, pp. 1–7
- [16] Keysight Technologies.: 'E8707a radar target simulator 76 GHz to 77 GHz'. Solution Brochure, October, 2016, pp. 1–4
- [17] Telemeter Electronic.: 'RTS-24G radar target simulator'. Solution Brochure, September 2014, pp. 1–2
- [18] Keycom Corp.: 'Active target simulator for collision avoidance radar (long range) radar test system', Available at <http://www.keycom.co.jp/e/products/rat/rat01/page2.html>, accessed February 28, 2018
- [19] konrad technologies.: 'A test solution for ADAS virtual test drive', Internet: <https://www.konrad-technologies.com/en/products/software/konrad-automotive-radar-test-system.html> accessed February 28, 2018
- [20] dSPACE GmbH.: 'Radar test bench with dSPACE SCALEXIO HIL system', Available at [https://www.dspace.com/en/pub/home/medien/videos/productvideos/video\\_radartestbench.cfm](https://www.dspace.com/en/pub/home/medien/videos/productvideos/video_radartestbench.cfm), accessed February 28, 2018
- [21] Keycom Corp.: 'Active target simulator for collision avoidance radar (long range), moving multiple target, multiple lane type', Available at <http://www.keycom.co.jp/e/products/rat/rat11/page.html>, accessed February 28, 2018
- [22] Gadringer, M., Metzner, S., Schreiber, H., *et al.*: 'Radar stimulation for a novel ADAS system'. Graz Symp. VIRTUAL VEHICLE, Graz, Austria, June 2017
- [23] Sanna, A.: 'Measurement of E.M. Radiation through different bumpers'. European Radar Conf., Workshop: Automotive Radar Measurement Solutions – For End-of-Line Purposes as well as in Aftersales, Nuremberg, Germany, October 2017, pp. 1–17
- [24] VIRES Simulationstechnologie GmbH.: 'VTD – virtual test drive', Available at <https://vires.com/vtd-vires-virtual-test-drive>, January 2018, accessed February 23, 2018
- [25] Ling, H., Chou, R.C., Lee, S.W.: 'Shooting and bounding rays: calculating the RCS of an arbitrarily shaped cavity', *IEEE Trans. Antennas Propag.*, 1989, 37, (2), pp. 194–205
- [26] Phong, B.T.: 'Illumination for computer generated pictures', *Commun. ACM*, 1975, 18, (6), pp. 311–317
- [27] Maier, F.M., Makkapati, V.M., Horn, M.: 'Adapting Phong into a simulation for stimulation of automotive radar sensors'. Int. Conf. Microwaves for Intelligent Mobility, Munich, Germany, April 2018
- [28] Richards, M.A., Holm, W.A., Scheer, J.: 'Principles of modern radar: basic principles' (Scitech Publishing, Edison, NJ, 2010)
- [29] ApisSys: 'AV104 radar emitter-receiver DRFM', Available at [http://www.apissys.com/views/media\\_produit/datasheets/6/Datasheet\\_AV104\\_Web-2.pdf](http://www.apissys.com/views/media_produit/datasheets/6/Datasheet_AV104_Web-2.pdf), accessed February 26, 2018